



VIBRATIONAL RESONANCE IN AN ASYMMETRIC DUFFING OSCILLATOR

S. JEYAKUMARI and V. CHINNATHAMBI
*Department of Physics, Sri K.G.S. Arts College,
Srivaikuntam 628 619, Tamilnadu, India*

S. RAJASEKAR
*School of Physics, Bharathidasan University,
Tiruchirapalli 620 024, Tamilnadu, India
rajasekar@cnd.bdu.ac.in*

M. A. F. SANJUAN
*Departamento de Física, Universidad Rey Juan Carlos,
Tulipán s/n, 28933 Móstoles, Madrid, Spain
miguel.sanjuan@urjc.es*

Received February 8, 2010; Revised April 7, 2010

We analyze how the asymmetry of the potential well of the Duffing oscillator affects the vibrational resonance. We obtain, numerically and theoretically, the values of the low-frequency and amplitude of the high-frequency forces at which vibrational resonance occurs. Furthermore, we observe that an additional resonance is induced by the asymmetry of the potential well. We account the additional resonance in terms of resonant frequency of the slow motion of the system. Resonance occurs in the asymmetric system for the input signal frequency range for which it is not possible in the symmetric system. Resonance is also studied with nonsinusoidal input signals and in the presence of additive Gaussian white noise.

Keywords: Vibrational resonance; asymmetric Duffing oscillator; biperiodic force.

1. Introduction

The study of the occurrence of vibrational resonance [Landa & McClintock, 2000; Gitterman, 2001] — a resonant dynamics induced by a high-frequency periodic force at the low-frequency ω of the input periodic signal — has received considerable interest in the past few years. In a typical bistable system when the amplitude g of a high-frequency periodic force is varied, the amplitude of the response at the low-frequency shows a bell-shape curve with a maximum enhancement of the response at a critical value denoted as g_{VR} . Experimental evidence of the vibrational resonance has been demonstrated in analog simulations of

the overdamped Duffing oscillator [Baltanas *et al.*, 2003], in an excitable electronic circuit with Chua's diode [Ullner *et al.*, 2003] and in a bistable optical cavity laser [Chizhevsky *et al.*, 2003]. A theoretical approach for vibrational resonance in the presence of additive white noise has also been developed [Casado-Pascual *et al.*, 2003]. A scaling-law relating the gain factor for the low-frequency signal due to vibrational resonance with the strength of the added noise was obtained based on an analytical treatment for an overdamped bistable system and verified experimentally in a vertical cavity surface emitting laser [Chizhevsky & Giacomelli, 2004; Chizhevsky, 2008]. Moreover, it has been

shown that vibrational resonance is an effective phenomenon to enhance the detection and recovery of weak aperiodic binary signals in stochastic bistable systems [Chizhevsky & Giacomelli, 2008]. Furthermore, multiple vibrational resonance in a monostable [Jeyakumari *et al.*, 2009a] and multistable [Jeyakumari *et al.*, 2009b] quintic oscillator and single resonance in coupled and small world networks of FitzHugh–Nagumo equations [Deng *et al.*, 2009; Deng *et al.*, 2010] were very recently reported.

Vibrational resonance has been studied in the overdamped bistable system with the asymmetric potential $V(x) = -(1/2)\alpha x^2 + (1/4)\beta x^4 - \gamma x$, $\alpha, \beta, \gamma > 0$ [Chizhevsky & Giacomelli, 2006] and with $V(x) = 4(x - x^3) + \Delta$ [Chizhevsky & Giacomelli, 2008] where Δ is a constant parameter describing the level of asymmetry. A single resonance is reported when the amplitude of the high-frequency force or Δ is varied. Our prime goal in the present paper is to report the result of a detailed theoretical and numerical analysis of the vibrational resonance in the asymmetric Duffing oscillator

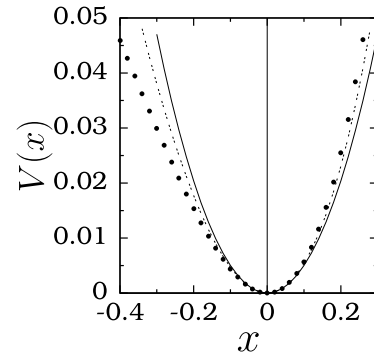
$$\ddot{x} + d\dot{x} + \frac{dV}{dx} = f \cos \omega t + g \cos \Omega t, \quad (1)$$

where $\Omega \gg \omega$ and the asymmetric potential of the system in the absence of damping and external force is

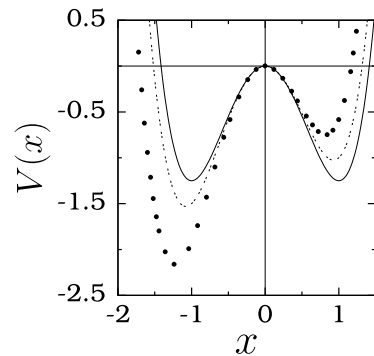
$$V(x) = \frac{1}{2}\omega_0^2 x^2 + \frac{1}{3}\alpha x^3 + \frac{1}{4}\beta x^4. \quad (2)$$

The potential $V(x)$ is symmetric when $\alpha = 0$. Figure 1 illustrates the influence of the asymmetric parameter α on the shape of the single-well and the double-well potentials. A two-state theory for stochastic resonance was developed for the overdamped system with the asymmetric potential (2) subjected to Gaussian [Wio & Bouzat, 1999; Li, 2002] and nonGaussian [Wio & Bouzat, 1999] noises. When the asymmetry parameter α is increased, weakening of stochastic resonance is observed. That is, signal-to-noise ratio is decreased and the optimum noise intensity at which stochastic resonance occurs is increased by the asymmetry. Recently, double stochastic resonance is reported in an overdamped system with a deformable asymmetric double-well potential [Borromeo & Marchesoni, 2010].

For $\Omega \gg \omega$, due to the difference in time scales of the low-frequency force $f \cos \omega t$ and the



(a)



(b)

Fig. 1. Shape of the potential $V(x)$ for (a) $\omega_0^2 = \beta = 1$ and $\alpha = 0$ (continuous line), 0.75 (dashed line), 1.9 (painted circles) and (b) $\omega_0^2 = -5, \beta = 5$ and $\alpha = 0$ (continuous line), 0.75 (dashed line), 2 (painted circles).

high-frequency force $g \cos \Omega t$, we assume that the solution of the system (1) consists of a slow motion $X(t)$ and a fast motion $\psi(t, \Omega t)$. Applying a theoretical approach, in a linear approximation, we obtain an analytical expression for the response amplitude Q of the low-frequency (ω) output signal. Using this theoretical expression of Q , we analyze the effect of the asymmetry parameter α on vibrational resonance. We obtain the theoretical values of ω and g at which vibrational resonance occurs when we have an asymmetry in both single-well and double-well cases. Our theoretical prediction is in good agreement with the numerical simulation. One main result is the occurrence of an additional resonance for a range of values of α in the asymmetric system compared to the symmetric system. We describe the single and multiple resonances in terms of resonant frequency of the linear version of the slow motion. It is worth noting that the number of resonances taking place for the sinusoidal input signal $f \cos \omega t$ persists when it is replaced by nonsinusoidal and

arbitrary shape binary signals of same frequency and amplitude. Strong degradation and suppression of resonance are found in large intensity of added Gaussian white noise. Additional resonance occurs in the overdamped version of the system (1) and in the damped asymmetric quintic oscillator also.

2. Theoretical Approach

For $\Omega \gg \omega$ we assume the solution of Eq. (1) as $x(t) = X(t) + \psi(t, \tau = \Omega t)$ where X and ψ are slow motion with period $2\pi/\omega$ and fast motion with period $2\pi/\Omega$, respectively. Because ψ is rapidly varying, we approximate the equation of motion for ψ as $\ddot{\psi} = g \cos \Omega t$ which gives $\psi = -(g/\Omega^2) \cos \Omega t$, $\psi_{av} = (1/2\pi) \int_0^{2\pi} \psi d\tau = 0$, $\psi_{av}^2 = g^2/2\Omega^4$ and $\psi_{av}^3 = 0$. Then the equation for the slow motion is

$$\ddot{X} + d\dot{X} + C_2X + \alpha X^2 + \beta X^3 + C_1 = f \cos \omega t, \quad (3)$$

where

$$C_1 = \frac{\alpha g^2}{2\Omega^4}, \quad C_2 = \omega_0^2 + \frac{3\beta g^2}{2\Omega^4}. \quad (4)$$

Equation (3) can be viewed as the equation of motion of a system with the effective potential

$$V_{\text{eff}}(X) = C_1X + \frac{1}{2}C_2X^2 + \frac{1}{3}\alpha X^3 + \frac{1}{4}\beta X^4. \quad (5)$$

Slow oscillations take place about the equilibrium points X^* which are roots of the cubic equation

$$\beta X^{*3} + \alpha X^{*2} + C_2X^* + C_1 = 0. \quad (6)$$

If Eq. (6) has three real roots, then we designate them as X_L^* , X_M^* and X_R^* with $X_L^* < X_M^* < X_R^*$. When V_{eff} becomes a double-well potential, then X_L^* and X_R^* are the local minimum of left- and right-wells respectively, while X_M^* is the local maximum of it.

Substituting $X = Y + X^*$, where Y is the deviation of the slow motion from X^* , in Eq. (3), we obtain

$$\ddot{Y} + d\dot{Y} + \omega_r^2 Y + \alpha' Y^2 + \beta Y^3 = f \cos \omega t, \quad (7)$$

where

$$\omega_r^2 = C_2 + 2\alpha X^* + 3\beta X^{*2}, \quad \alpha' = \alpha + 3\beta X^*. \quad (8)$$

The solution of the linear version of Eq. (7) in the limit $t \rightarrow \infty$ and $f \ll 1$ is $A_L \cos(\omega t - \phi)$ where

$$A_L = \frac{f}{[(\omega_r^2 - \omega^2)^2 + d^2\omega^2]^{1/2}}, \quad (9)$$

$$\phi = \tan^{-1} \left(\frac{\omega^2 - \omega_r^2}{d\omega} \right).$$

The response amplitude Q is A_L/f , where ω_r is the resonant frequency of the linear version of the equation of motion of the slow variable $X(t)$.

3. Resonance in the System with an Asymmetric Single-Well Potential

The shape of the potential $V(x)$ depends basically on the parameters ω_0^2 , α and β . $V(x)$ is asymmetric due to the term $(1/3)\alpha x^3$. For $\omega_0^2, \alpha, \beta > 0$ the potential $V(x)$ has a single-well form [Fig. 1(a)] for $\alpha^2 < 4\omega_0^2\beta$ and double-well form for $\alpha^2 > 4\omega_0^2\beta$. When $\omega_0^2 < 0, \beta > 0, \alpha$ -arbitrary $V(x)$ becomes a double-well potential [Fig. 1(b)]. In this section, we analyze the occurrence of vibrational resonance in the system (1) with the single-well potential shown in Fig. 1(a).

For a single-well system (1), Eq. (3) with $f = 0$ has only one equilibrium point X^* . When $\alpha = 0$, X^* is always 0. $X^* < 0$ for $\alpha > 0$ while $X^* > 0$ for $\alpha < 0$. $V_{\text{eff}}(X)$ remains as a single-well potential. The values of the control parameter at which resonance occurs correspond to the minima of $S = (\omega_r^2 - \omega^2)^2 + d^2\omega^2$.

For a fixed value of ω when g is varied, resonance occurs at $g = g_{\text{VR}}$ where g_{VR} is a root of $S_g = dS/dg = 4(\omega_r^2 - \omega^2)\omega_r\omega_{rg} = 0$ and $S_{gg}|_{g=g_{\text{VR}}} = 8\omega\omega_{rg}^2 > 0$. Here $\omega_{rg} = d\omega_r/dg$. For $\alpha = 0$ we obtain

$$g_{\text{VR}} = \Omega^2 \sqrt{\frac{2(\omega^2 - \omega_0^2)}{3\beta}}. \quad (10)$$

For $\omega^2 < \omega_0^2$, resonance will not occur if the control parameter g is varied from 0. In the asymmetric system ($\alpha \neq 0$), $X^* \neq 0$ and ω_r is a complicated function of the parameters. Analytical expression for g_{VR} is difficult to find. However, we can determine g_{VR} from S by numerically finding the roots of $S_g = 0$ and the value of S_{gg} at the roots.

We choose the values of the parameters as $\omega_0^2 = 1, \beta = 1, d = 0.3, f = 0.05, \Omega = 10$. $V(x)$ is a single-well potential for $0 < \alpha < 2$ and a double-well potential for $\alpha > 2$. We consider now the case $0 < \alpha < 2$. Figure 2 shows both theoretically and numerically computed g_{VR} as a function of ω for $\alpha = 0, 1$ and 1.9 . From the numerical solution $x(t)$

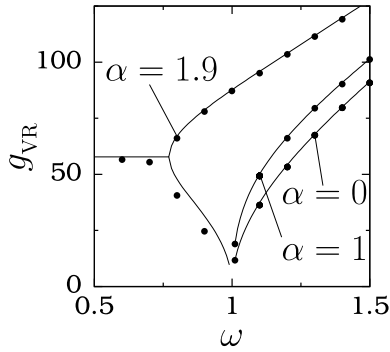


Fig. 2. Variation of g_{VR} with ω for three values of α . The potential is symmetric for $\alpha = 0$. The continuous line is the theoretical prediction of vibrational resonance while the painted circle represents the value of g_{VR} calculated from the numerical solution of the system.

of Eq. (1), the sine and cosine components Q_S and Q_C are calculated from the equations

$$Q_S = \frac{2}{nT} \int_0^{nT} x(t) \sin \omega t dt, \quad (11a)$$

$$Q_C = \frac{2}{nT} \int_0^{nT} x(t) \cos \omega t dt, \quad (11b)$$

where $T = 2\pi/\omega$ and n is taken as 500. Then $Q = \sqrt{Q_S^2 + Q_C^2}/f$. From the numerically computed Q versus g the value of g_{VR} at which Q becomes maximum is found. The theoretical approximation is in good agreement with the numerical result. We notice the absence of resonance for $\omega < 1$ in Fig. 2, for $\alpha = 0$. That is, in the symmetric system if $\omega < 1$ ($= \omega_0^2$) an enhancement of the amplitude of the signal at low-frequency ω is not possible when the amplitude g of high-frequency force is varied.

This is the case for $0 < \alpha < 1.23$. In this interval of α , ω_r increases monotonically with g from the value 1 and hence no resonance appears for $\omega < 1$. An interesting result is the observation of double resonance for $\alpha \in [1.23, 2]$. As shown in Fig. 2 for $\alpha = 1.9$, double resonance occurs when g is varied from zero for each fixed value of $\omega \in [0.7721, 1]$.

We explain the g_{VR} versus ω curve for $\alpha = 1.9$ with the plot of ω_r versus g [Fig. 3(a)] and ω_{rg} versus g [Fig. 3(b)]. From Figs. 3(a) and 3(b) we infer the following:

- (i) For $0 < \omega < \omega_{r1} = 0.7721$ the value of ω_r is greater than ω and $\omega_r^2 - \omega^2$ in the function S or Q is nonzero for any value of g . However, $\omega_{rg} = 0$ at $g_0 = 57.8$. Since $S_g = 4(\omega_r^2 - \omega^2)\omega_r\omega_{rg}$ the function S becomes a minimum at this value of g . Hence, there is a resonance at $g = g_0$ for $0 < \omega < \omega_{r1}$. In Fig. 3(c), for $\omega = 0.5$, as g increases from 0, the value of Q increases, reaches a maximum value at $g = g_{VR} = g_0$ and then decreases with further increase in g . For $0 < \omega < \omega_{r1}$, g_{VR} remains a constant because ω_r is independent of ω and $\omega_r^2 - \omega^2 \neq 0$.
- (ii) Corresponding to each value of g in the interval $[0, g_0]$, there is another value of g in the interval $[g_0, g_1 = 88]$ both having the same value of ω_r . Consequently, for each fixed value of $\omega \in [\omega_{r1}, \omega_{r2} = 1]$, the quantity $\omega_r^2 - \omega^2$ is 0 for two values of g . Hence, there are two resonances. In the symmetric single-well system only one resonance is possible and is given by Eq. (10). The additional resonance is due to the asymmetry introduced in the system. We can see a double resonance for $\omega = 0.85$ and $\omega = 0.9$ in Fig. 3(c). The value of Q is the

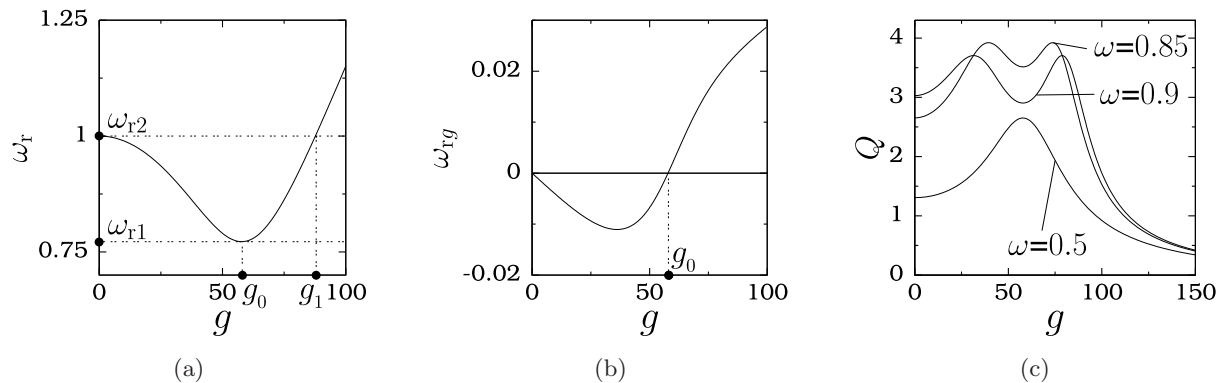


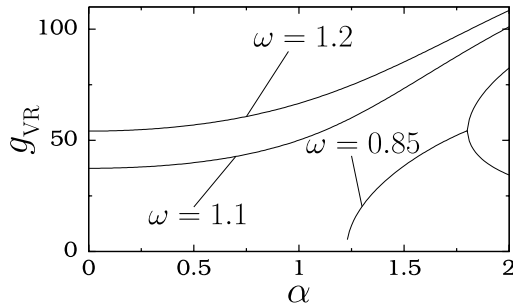
Fig. 3. (a) Variation of resonant frequency ω_r with g for $\alpha = 1.9$. ω_r is independent of ω . (b) ω_{rg} ($= d\omega_r/dg$) versus g for $\alpha = 1.9$. ω_r and ω_{rg} are calculated from Eq. (8). (c) Numerically computed Q versus g for the system (1) with single-well potential for three values of ω . The values of the other parameters are $\omega_0^2 = 1, \beta = 1, \alpha = 1.9, d = 0.3, f = 0.05$ and $\Omega = 10$.

same at both resonances since they are due to $\omega_r^2 - \omega^2 = 0$ and Q_{\max} is $1/(d\omega)$. On the other hand, the influence of damping is to reduce the value of Q and it does not alter the value of g_{VR} .

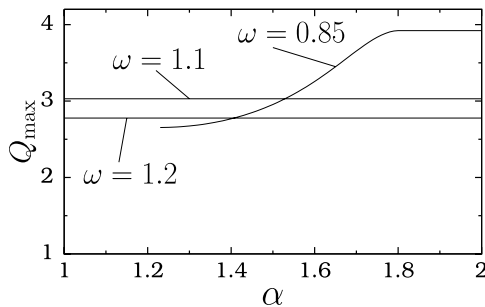
- (iii) When $\omega > \omega_{r2}$ then $\omega_r^2 - \omega^2 = 0$ for a value of $g > g_1$ and hence there is a resonance.

For $\omega > \omega_{r1}$ the resonance is due to the matching of the resonant frequency ω_r with the frequency ω of the input signal while for $0 < \omega < \omega_{r1}$ though $\omega_r \neq \omega$ a resonance occurs due to the minimization of the function S .

A plot of g_{VR} versus α and Q_{\max} versus α for three values of ω is shown in Fig. 4. Note also that a resonance does not occur in the symmetric case for $\omega = 0.85$ when g is varied. When asymmetry is introduced the absence of resonance continues for values of $\alpha < 1.23$. Single and double resonances take place for $1.23 \leq \alpha < 1.81$ and $1.81 \leq \alpha \leq 2$, respectively. For $\omega > 1$, a single resonance occurs for $0 < \alpha < 2$. This is shown in Fig. 4(a) for $\omega = 1.1$ and 1.2 . In Fig. 4(b) the reason for the constancy of Q_{\max} with α is that the associated resonance is due to $\omega_r = \omega$. The variation of Q_{\max} with α (in the interval $1.23 \leq \alpha < 1.81$ for $\omega = 0.85$) indicates



(a)



(b)

Fig. 4. Plots of g_{VR} and Q_{\max} (at $g = g_{\text{VR}}$) as a function of ω .

that the resonance is due to the minimization of S with $\omega_r \neq \omega$.

Besides this previous analysis, we also consider the effect of α on the vibrational resonance by using nonsinusoidal and arbitrary binary shape periodic input signals. We consider the following periodic signals in place of $f \cos \omega t$:

$$h_1(t) = f \begin{cases} \cos \omega t, & 0 \leq t < \frac{\pi}{\omega} \\ \frac{2\omega}{\pi}t - 3, & \frac{\pi}{\omega} \leq t < \frac{2\pi}{\omega} \end{cases} \quad (12)$$

$$h_2(t) = f \begin{cases} \frac{\omega}{\pi}t - \frac{1}{2}, & 0 \leq t < \frac{\pi}{\omega} \\ -\frac{\omega}{\pi}t + \frac{3}{2}, & \frac{\pi}{\omega} \leq t < \frac{2\pi}{\omega} \end{cases} \quad (13)$$

$$h_3(t) = f \begin{cases} 1, & 0 \leq t < \frac{\pi}{4\omega} \\ -0.5, & \frac{\pi}{4\omega} \leq t < \frac{3\pi}{4\omega} \\ 0.5, & \frac{3\pi}{4\omega} \leq t < \frac{\pi}{\omega} \\ -0.75, & \frac{\pi}{\omega} \leq t < \frac{5\pi}{4\omega} \\ 1, & \frac{5\pi}{4\omega} \leq t < \frac{7\pi}{4\omega} \\ -0.25, & \frac{7\pi}{4\omega} \leq t < \frac{2\pi}{\omega}. \end{cases} \quad (14)$$

In all the above three signals $t = \text{mod}(2\pi/\omega)$. Figure 5 shows the numerically calculated Q versus g for $\alpha = 1.9$ with the different input signals with the same frequency $\omega = 0.85$ and amplitude $f = 0.05$. The high-frequency force is again $g \cos \Omega t$. In all the cases, a double resonance is observed. g_{VR} values for the signals $f \cos \omega t$, $h_1(t)$, $h_2(t)$ and $h_3(t)$ are (34, 72), (38, 80), (95, 177) and (42, 71) respectively. The effect of asymmetry is similar for all the forms of the periodic input signals considered. The above result indicates that the form of the high-frequency force need not be the same as the input signal. For any arbitrary periodic signal of frequency ω , amplification of the amplitude of the output signal at the frequency ω can be carried out by using the force $g \cos \Omega t$.

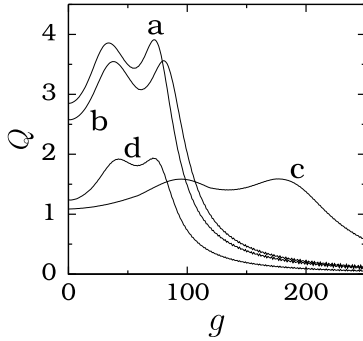


Fig. 5. Q versus g for the system (1) with the low-frequency signal being (a) $f \cos \omega t$, (b) $h_1(t)$, (c) $h_2(t)$ and (d) $h_3(t)$. The high-frequency force is $g \cos \Omega t$. The values of the parameters are $\omega_0^2 = 1$, $\beta = 1$, $d = 0.3$, $f = 0.05$, $\omega = 0.85$, $\alpha = 1.9$ and $\Omega = 10$.

Next, we illustrate the effect of additive Gaussian white noise $\eta(t)$, with zero mean and the correlation function $\langle \eta(t)\eta(t + \tau) \rangle = D\delta(t - \tau)$ where D is the variance or intensity of the noise, in the system (1) with double resonance. In the numerical calculation of Q , 2×10^3 trajectories, $x^{(i)}(t)$, are generated by numerically integrating the equation of motion for every realization of the noise $\eta(t)$. We use the same initial condition for all the trajectories. First 500 drive cycles of low-frequency force are left as transient. After every integration step we calculate $\langle x(t) \rangle$, the average of all $x^{(i)}(t)$. This average quantity is used in Eqs. (11) for the calculation of Q . In Fig. 6 numerically calculated Q versus g is plotted for four values of noise intensity along with the noise free resonance curve. Double resonance with slight shift in the values of g_{VR} is observed for small values of D . In Fig. 6 we notice the following:

- (i) An increase in the noise intensity first suppresses the resonance occurring at a lower

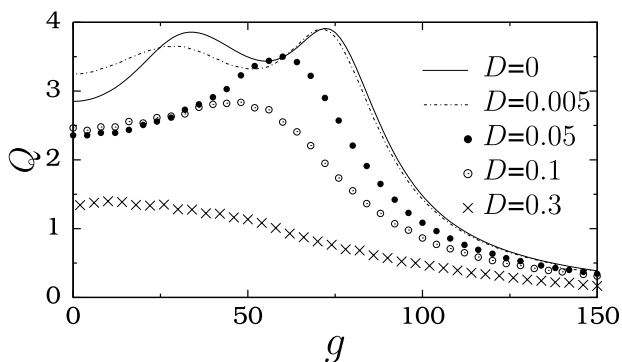


Fig. 6. Response amplitude Q versus the amplitude g of the high-frequency force in the absence of external noise and for four fixed values of the noise intensity D with $\omega = 0.85$ and $\alpha = 1.9$.

value of the amplitude of the high-frequency force followed by the other resonance.

- (ii) The value of g_{VR} moves towards the origin with D . The Gaussian white noise contains all the frequencies. As pointed out in [Baltanas *et al.*, 2003; Casado-Pascual *et al.*, 2003], the portion of the noise corresponding to the high-frequency interval is the source for the decrease in the value of g_{VR} .
- (iii) Q , specifically Q_{max} , decreases when D increases. The part of noise with frequencies other than the high-frequency region degrades the performance of the system by decreasing the value of Q .

4. Resonance in an Asymmetric Double-Well System

The potential $V(x)$ has an asymmetric double-well shape for $\omega_0^2 < 0$, $\beta > 0$ and α -arbitrary [Fig. 1(b)]. As α increases from zero (i) the depth of the left-well increases while that of the right-well decreases and (ii) the location of the local minimum of the right-well moves towards the origin whereas the minimum of the left-well moves further away from the origin.

We fix the values of the parameters as $\omega_0^2 = -5$, $\beta = 5$, $d = 0.3$, $f = 0.05$, $\omega = 1.5$ and $\Omega = 10$. For $\alpha = 0$, from Eq. (6) with $C_1 = 0$, we find that the system (3) in the absence of low-frequency force has two stable and one unstable equilibrium points for $g < g_c = 81.65$. There is only one equilibrium point for $g \geq g_c$ and V_{eff} is a single-well potential. As shown in Fig. 7 the bifurcation is of pitchfork type. For $\alpha \neq 0$ saddle-node bifurcation occurs and is shown in Fig. 7 for $\alpha = 0.75$. As g increases from 0 the two stable equilibrium points move toward the

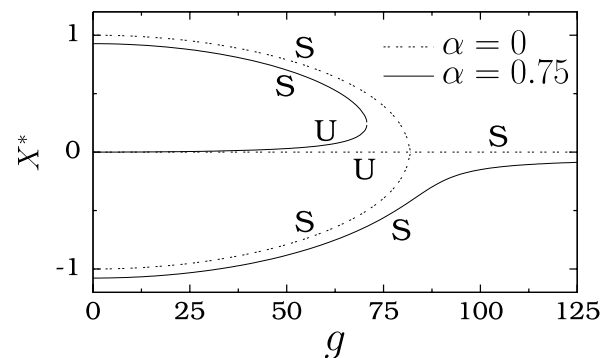


Fig. 7. X^* versus g of the system (3) in the absence of low-frequency force for $\alpha = 0$ and $\alpha = 0.75$. S and U denote stable and unstable branches respectively of the equilibrium points.

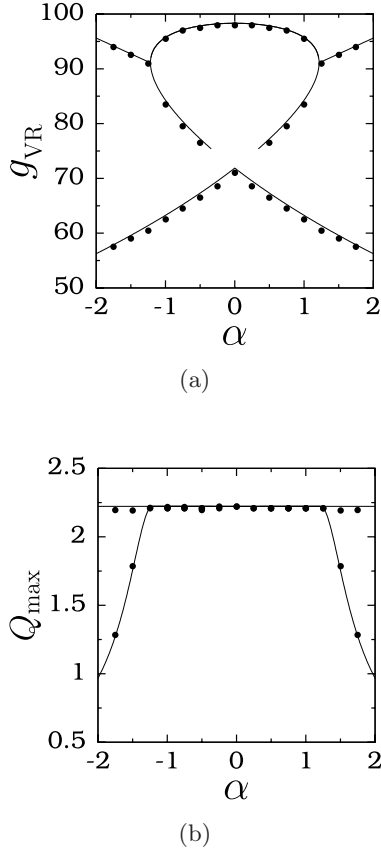


Fig. 8. Plots of (a) theoretical and numerical g_{VR} versus α and (b) Q_{max} ($g = g_{VR}$) versus α for the double-well case of the system (1). Here $\omega_0^2 = -5, \beta = 5, d = 0.3, f = 0.05, \omega = 1.5, \Omega = 10$. g_{VR} and Q_{max} are symmetric about $\alpha = 0$. The continuous line and the painted circles represent the theoretical and numerical results, respectively.

origin while the unstable one moves away from the origin along the positive X -axis. At $g = g_c = 70.72$ the two equilibrium points lying in the region $X > 0$ collide with each other and disappear. For $g \geq g_c$ there is only one stable equilibrium point and is in the region $X < 0$. This is the case for $\alpha > 0$. For $\alpha < 0$ the stable equilibrium point in the region $X > 0$ remains stable while the other stable equilibrium point in the region $X < 0$ collides with the unstable point and both disappear at $g = g_c$. That is, the high-frequency periodic modulation with amplitude $g > g_c$ leads to the elimination of bistability.

The effect of α on g_{VR} and Q_{max} (the value of Q at $g = g_{VR}$) is depicted in Fig. 8. We have chosen the stable equilibrium point X_R^* (X_L^*), which is the local minimum of the lower depth well, when the effective potential is a double-well in order to obtain this figure for $\alpha > 0$ ($\alpha < 0$), in the theoretical calculation of g_{VR} . (For $\alpha > 0$ (< 0) the right (left)-well has a lower depth than the other well.)

In the numerical simulation, the above refers to the choice of the orbit confined to the lower depth well for the starting small value of g . If the system is considered with the orbit confined to higher depth well for the starting small value of g for each fixed value of α , then g_{VR} versus α plot is the same as Fig. 8(a) except without the lower branch ($g_{VR} \leq 70$).

Observe that g_{VR} and Q_{max} are symmetric about $\alpha = 0$, as shown in Fig. 8. For $|\alpha| \in [0.34, 1.23]$ three resonances occur while for the remaining values of α two resonances occur. We can account the various branches in Fig. 8 with ω_r versus g plot [Fig. 9(a)]. In Fig. 9(a) when $\alpha = 0$ as g increases the value of ω_r decreases and becomes ≈ 0 at $g_c = 81.65$ and then increases.

As seen in Fig. 7 at $g = g_c$ a pitchfork bifurcation occurs and the double-well shape of V_{eff} becomes a single-well. Furthermore, X_R^* (as well as X_L^*) $\rightarrow 0$ as $g \rightarrow g_c$ and $X^* = 0$ is the only possible equilibrium state for which a slow oscillation takes place. There is no abrupt change in the value

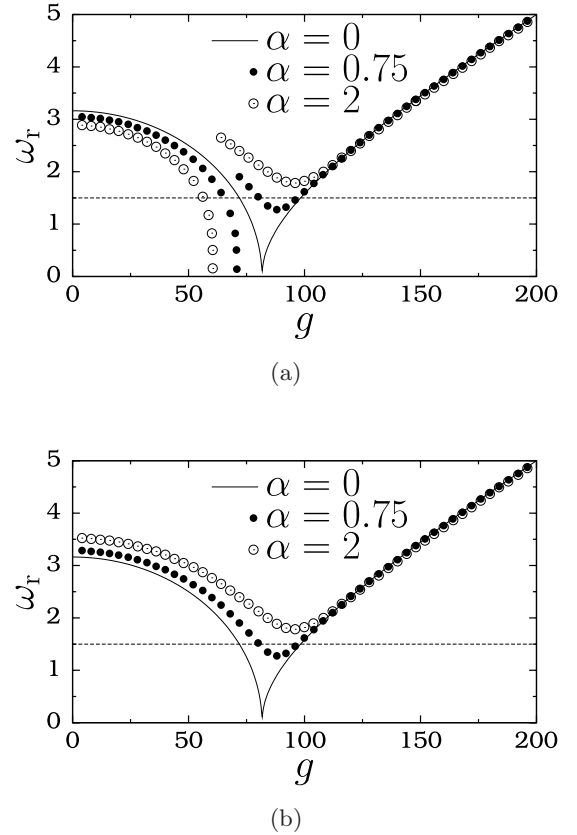


Fig. 9. Theoretical resonant frequency ω_r as a function of g for three values of the asymmetry parameter α . The horizontal dashed line corresponds to $\omega_r = \omega = 1.5$. In the subplots (a) and (b) X^* in Eq. (8) is chosen as X_R^* and X_L^* , respectively.

of ω_r at $g = g_c$. Since ω_r is independent of ω , for each value of ω in the interval $0 < \omega < \omega_r(g = 0)$, $\omega_r = \omega$ at two values of g and hence there are two resonances. A numerically computed Q is plotted as a function of g for three values of α in Fig. 10(a), where for the starting small value of g an initial condition on the orbit confined to right-well is chosen. We notice two resonances at $g_{VR} = 71.05$ and 98 for $\alpha = 0$.

g_c and $\omega_r(g = 0)$ depend on the value of α . For $\alpha = 0.75$ as g increases from 0 the value of ω_r decreases and reaches the minimum value 0 in the limit $g \rightarrow g_c = 70.72$. At this value of g the effective potential undergoes bifurcation to a single-well form. The point is that for $g < g_c$ two slow motions coexist while for $g \geq g_c$ only one slow motion exists and is about $X_L^* < 0$. Moreover, as $g \rightarrow g_c$, we do not have either the case X_L^* and $X_R^* \rightarrow X^* = 0$ (as is the case for $\alpha = 0$) or $X_L^* \rightarrow X_R^*$. Consequently, the resonant frequency at $g = g_c$ jumps from the minimum value 0 to a higher value corresponding to the slow motion about X_L^* . This is the reason for the appearance of discontinuity in Q versus g plot in Fig. 10(a). If $X^* = X_L^*$ is used in the theoretical calculation of ω_r given by Eq. (8) for both $g < g_c$ and $g > g_c$, then we get the ω_r versus g as shown in Fig. 9(b) where we can notice a smooth variation of ω_r at $g = g_c$.

An interesting observation in Fig. 9(a) is that the dashed horizontal line corresponding to $\omega = 1.5$ intersects the ω_r curve at three values of g . That is, $\omega_r^2 - \omega^2 = 0$ for three values of g . These values of g are $g_{VR} = 64.35, 79.55$ and 96.85 — one lies below g_c while the other two are above g_c . At all these three resonances $Q_{max} = 1/(d\omega) = 2.22222$. This is the case for $\alpha \in [0.34, 1.23]$. For each fixed value of α in this interval, resonance occurs at three different values of g and the values of g_{VR} vary with α . However, Q_{max} at the three values of g_{VR} remain equal and even for all values of α in the above interval. Moreover, it depends only on the parameters d and ω and independent of other parameters. We can observe three resonances all with the same Q in Fig. 10(a), for $\alpha = 0.75$. The occurrence of three resonances is attributable to the tuning of three different oscillations: one confined to the lower depth well, second confined to the higher depth well and the third involving cross-well motion. In the symmetric double-well system ω_r of the two intra-well, oscillations are the same and hence only one resonance for $g < g_c$ (and another for $g > g_c$, associated with cross-well motion). In the asymmetric

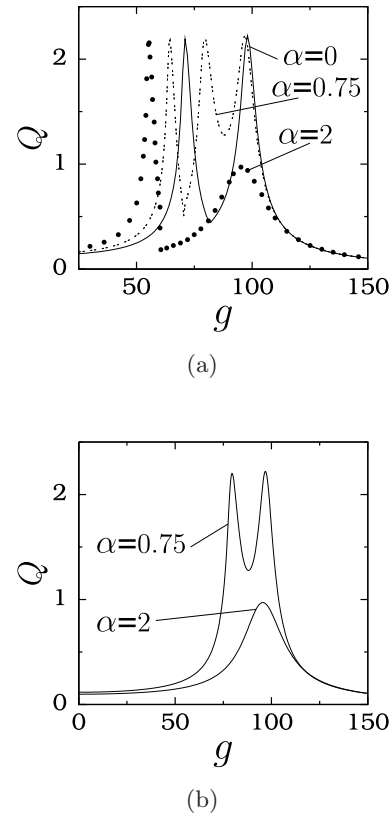


Fig. 10. Numerically calculated response amplitude Q versus g for three values of α of the system (1) with a double-well potential $V(x)$. For the starting value of g the initial condition is chosen on the orbit confined to (a) right-well and (b) left-well of the system.

double-well case ω_r of the two intra-well, oscillations are different (as shown in Fig. 9). The response curve for $\alpha = 0.75$ in Fig. 10(a) can be compared with the response curve shown in Fig. 10(b), where the initial condition for the starting small value of g is on the orbit confined to the left-well. In Fig. 10(b) we notice only two resonances. The resonance at $g_{VR} = 64.35$ is absent.

When $\alpha = 2$, the $\omega = 1.5$ line in Fig. 9(a) intersects the resonant frequency curve only at $g = 55.25$. Q is maximum at this value of g with $\omega_r^2 - \omega^2 = 0$ and $Q_{max} = 1/(d\omega) = 2.22222$. For $g > g_c = 60.47$, ω_r curve has a local minimum at $g = 95.55$ and hence Q becomes a maximum though $\omega_r^2 - \omega^2 \neq 0$. The value of Q at this resonance is lower than its value at $g = 55.25$. For $\alpha = 2$ there are two resonances as shown in Fig. 10(a). For the same value of α in Fig. 10(b) we find only the second resonance. For $|\alpha| < 1.23$ all the resonances are due to $\omega_r^2 - \omega^2 = 0$ and hence $Q_{max} = 2.22222$ as seen in Fig. 8(b). In the remaining interval of α , one resonance is due to $\omega_r^2 - \omega^2 = 0$ while the other is

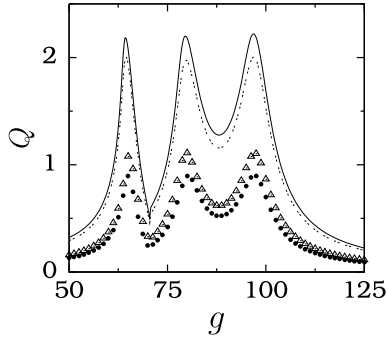


Fig. 11. Q versus g for different types of low-frequency input signal. The continuous line, dashed line, painted circles and triangles correspond to the signals $f \cos \omega t$, $h_1(t)$, $h_2(t)$ and $h_3(t)$ respectively, described in Eqs. (12)–(14).

due to the local minimum of ω_r with $\omega_r \neq \omega$ and hence there are two branches of Q_{\max} curve.

Figure 11 presents the variation of Q with g for the nonsinusoidal periodic signals given by Eqs. (12)–(14) for $\alpha = 0.75$ and $\omega = 1.5$. All the three resonances observed for the sinusoidal signal $f \cos \omega t$ persist for the other three forms of the periodic signal, however, with a slight shift in the values

of $g_{\text{VR}} \cdot Q_{\max}$ is also found to be different for the different signals. The decrease in the value of Q for the nonsinusoidal signal is due to the fact that they can be written as a Fourier series in terms of the sinusoidal terms with the fundamental frequency ω and its higher-order harmonics. Therefore, the value of Q at ω of the nonsinusoidal signal is lower than that of the sinusoidal signal $f \cos \omega t$.

The effect of additive Gaussian white noise on the resonance is also studied for $\alpha = 0.75$ and $\omega = 1.5$. The increase in the noise intensity is found to suppress the noise-free three resonances one by one. Moreover, the value Q_{\max} at the resonance(s) is decreased by the added noise, and for a sufficiently large noise intensity all the resonances are suppressed.

5. Resonance in the Overdamped System

The equation of motion of the overdamped version of the asymmetric Duffing oscillator is

$$\dot{x} = -\omega_0^2 x - \alpha x^2 - \beta x^3 + f \cos \omega t + g \cos \Omega t. \quad (15)$$

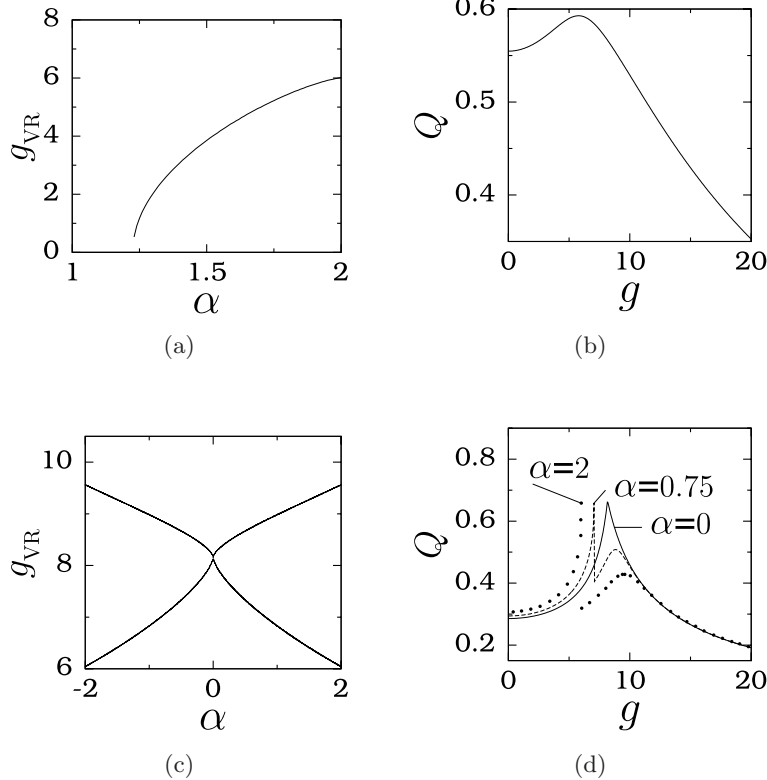


Fig. 12. (a) α versus g_{VR} for a single-well case of the overdamped system (15). The values of the parameters are $\omega_0^2 = 1$, $\beta = 1$ and $\Omega = 10$. (b) Q versus g for the single-well case with $\alpha = 1.9$, $f = 0.05$ and $\omega = 0.85$. (c) and (d) are for a double-well case where $\omega_0^2 = -5$, $\beta = 5$, $\Omega = 10$, $f = 0.05$ and $\omega = 1.5$.

The amplitude A_L of the low-frequency oscillation of the system (15) is obtained as

$$A_L = \frac{f}{\sqrt{\omega_r^2 + \omega^2}}, \quad (16)$$

where ω_r^2 is given by Eq. (8) and C_1 and C_2 in Eq. (6) now become

$$C_1 = \frac{\alpha g^2}{2\Omega^2}, \quad C_2 = \omega_0^2 + \frac{3\beta g^2}{2\Omega^2}. \quad (17)$$

For the system (15) with symmetric single-well ($\omega_0^2, \beta > 0, \alpha = 0$) as g increases ω_r^2 increases from ω_0^2 monotonically and hence there is no resonance. Resonance occurs in the asymmetric system for a range of values of α . For example, Fig. 12(a) shows g_{VR} versus α for $\omega_0^2 = 1, \beta = 1$ and $\Omega = 10$. As shown in Fig. 12(b), for $\omega = 0.85, f = 0.05$ and $\alpha = 1.9$ resonance takes place at $g = 5.78$. In the symmetric double-well case for $\omega_0^2 = -5, \beta = 5$ and $\Omega = 10$ only one resonance is possible ($g_{VR} = [2|\omega_0^2|\Omega^2/(3\beta)]^{1/2}$) and it occurs at $g = 8.165$. In Fig. 12(c) we notice two resonances for all nonzero values of the asymmetry parameter α . However, similar to the system (1) in the system (15) also

the value of Q_{max} at one resonance (which occurs at the minimum of the function S with $\omega_r^2 - \omega^2 \neq 0$ for the damped system and $\omega_r^2 \neq 0$ for the over-damped system) decreases with increase in α [see Fig. 12(d)].

6. Resonance in the Asymmetric Quintic Oscillator

The additional resonance found in the systems (1) and (15) due to the presence of asymmetry in the potential can be observed in other nonlinear asymmetric systems also. For example, consider the equation of motion of the asymmetric quintic oscillator driven by two periodic forces given by

$$\ddot{x} + d\dot{x} + \omega_0^2 x + \alpha x^2 + \beta x^3 + \gamma x^5 = f \cos \omega t + g \cos \Omega t. \quad (18)$$

When $\alpha = 0$, the potential of the quintic oscillator is symmetric. For $\omega_0^2, \alpha, \beta, \gamma > 0$ the potential is a single-well with a local minimum at $x = 0$. We fix the parameters as $\omega_0^2 = \beta = \gamma = 1, d = 0.3, f = 0.05, \omega = 1.25$ and $\Omega = 10$. Figure 13(a) shows the plot of g_{VR} versus α . When $\alpha = 0$ there

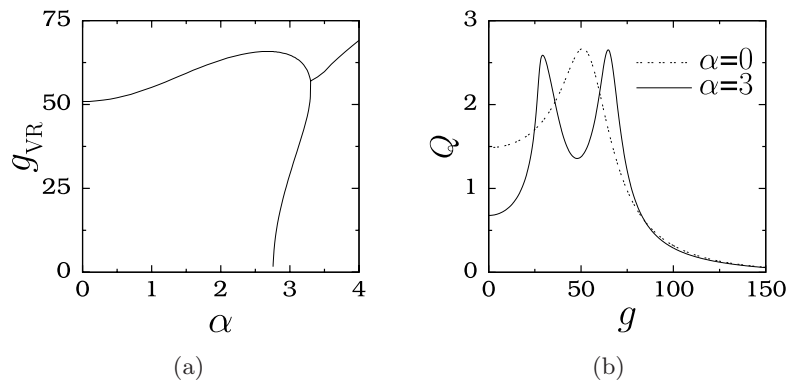


Fig. 13. (a) Plot of g_{VR} versus the asymmetry parameter α of the system (18) with a single-well potential. (b) Response amplitude Q as a function of g for $\alpha = 0$ and 3. $g_{VR} = 51$ when $\alpha = 0$. $g_{VR} = 29.25$ and 64.75 when $\alpha = 3$.

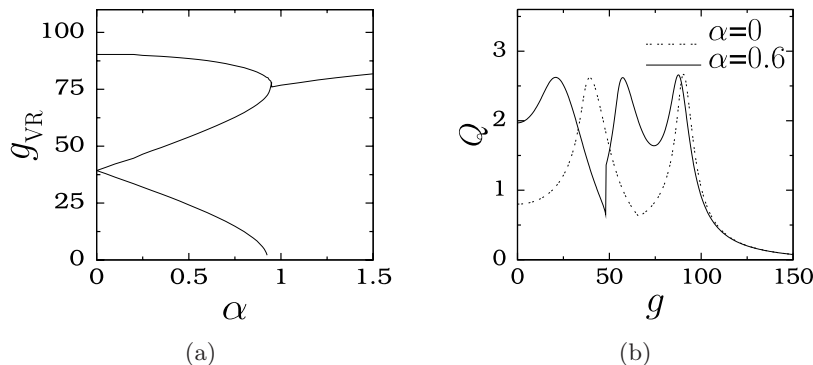


Fig. 14. (a) Plot of g_{VR} versus α for the system (18) with a double-well potential. (b) Q versus g for two values of α .

is only one resonance. Asymmetry induced second resonance occurs for $\alpha \in [2.75, 3.3]$. In Fig. 13(b) for $\alpha = 3$ we can clearly see two resonances.

The quintic oscillator has a double-well shape for $\omega_0^2 < 0$, $\beta, \gamma > 0$. We choose $\omega_0^2 = -1$ and the values of the other parameters as fixed earlier. In Fig. 14(a) g_{VR} versus α is plotted. As shown in Fig. 14(b) two resonances occur for $\alpha = 0$. One more resonance is found for $\alpha < 0.925$. An example is shown in Fig. 14(b) for $\alpha = 0.6$. For $\alpha > 0.925$ only one resonance occurs.

7. Conclusion

We have studied the occurrence of vibrational resonance in the asymmetric Duffing oscillator. When the asymmetry parameter α is varied, the depth of the two wells as well as the location of the local minima of the wells change. The introduction of the effective potential for the slow motion allowed us to find an approximate analytical expression for the response amplitude Q at the low-frequency ω . Multiple resonance is found for a range of fixed parameter values when the amplitude g of the high-frequency force is varied. In the symmetric single-well and double-well cases at most single and double resonances respectively are possible. We have shown the occurrence of an additional resonance due to the presence of the asymmetry in the potential. In the double-well system, the additional resonance appears when the orbit confined to the lower depth well is chosen for the starting small value of the control parameter g . The additional resonance is found in the overdamped system also. Importantly, in the overdamped symmetric single-well system vibrational resonance is not possible while it occurs for a range of values of the asymmetry parameter.

It is noteworthy to compare the effect of the asymmetry on stochastic resonance reported in [Wio & Bouzat, 1999; Li, 2002] with the vibrational resonance. These two resonances with $+\alpha$ are the same as $-\alpha$. Stochastic resonance does not occur with additive Gaussian noise in the single-well asymmetric system whereas vibrational resonance including double resonance takes place. In the double-well system, only one stochastic resonance is realized. Moreover, the asymmetry is found to increase the value of the optimum noise intensity at which resonance occurs and reduces the maximum value of signal-to-noise ratio. In contrast to this, we notice (i) more than one vibrational resonance in both damped system (Fig. 8)

and overdamped system [Fig. 12(c)] and (ii) for one resonance $g_{\text{VR}}(\alpha) < g_{\text{VR}}(\alpha = 0)$ and at this resonance $Q(\alpha, g_{\text{VR}}) = Q(\alpha = 0, g_{\text{VR}})$ for a range of values of α .

Acknowledgments

The work of S. Rajasekar forms part of a Department of Science and Technology, Government of India sponsored research project. M. A. F. Sanjuan acknowledges financial support from the Spanish Ministry of Education and Science under Project No. FIS2006-08525 and from the Spanish Ministry of Science and Innovation under Project No. FIS2009-09898.

References

- Baltanas, J. P., Lopez, L., Blechman, I. I., Landa, P. S., Zaikin, A., Kurths, J. & Sanjuan, M. A. F. [2003] "Experimental evidence, numerics, and theory of vibrational resonance in bistable systems," *Phys. Rev. E* **67**, 066119-1-7.
- Borromeo, M. & Marchesoni, F. [2010] "Double stochastic resonance over an asymmetric barrier," *Phys. Rev. E* **81**, 012102-1-4.
- Chizhevsky, V. N., Smeu, E. & Giacomelli, G. [2003] "Experimental evidence of vibrational resonance in an optical system," *Phys. Rev. Lett.* **91**, 220602-1-4.
- Chizhevsky, V. N. & Giacomelli, G. [2004] "Experimental and theoretical study of the noise-induced gain degradation in vibrational resonance," *Phys. Rev. E* **70**, 062101-1-4.
- Chizhevsky, V. N. & Giacomelli, G. [2006] "Experimental and theoretical study of vibrational resonance in a bistable system with asymmetry," *Phys. Rev. E* **73**, 022103-1-4.
- Chizhevsky, V. N. [2008] "Analytical study of vibrational resonance in an overdamped bistable oscillator," *Int. J. Bifurcation and Chaos* **18**, 1767–1773.
- Chizhevsky, V. N. & Giacomelli, G. [2008] "Vibrational resonance and the detection of aperiodic binary signals," *Phys. Rev. E* **77**, 051126-1-7.
- Deng, B., Wang, J. & Wei, X. [2009] "Effect of chemical synapse on vibrational resonance in coupled neurons," *Chaos* **19**, 013117-1-6.
- Deng, B., Wang, J., Wei, X., Tsang, K. M. & Chan, W. L. [2010] "Vibrational resonance in neuron populations," *Chaos* **20**, 013113-1-7.
- Gitterman, M. [2001] "Bistable oscillator driven by two periodic fields," *J. Phys. A: Math. Gen.* **34**, L355–L357.
- Jeyakumari, S., Chinnathambi, V., Rajasekar, S. & Sanjuan, M. A. F. [2009a] "Single and multiple vibrational resonance in a quintic oscillator with monostable potentials," *Phys. Rev. E* **80**, 046608-1-8.

- Jeyakumari, S., Chinnathambi, V., Rajasekar, S. & Sanjuan, M. A. F. [2009b] "Analysis of vibrational resonance in a quintic oscillator," *Chaos* **19**, 043128-1-8.
- Landa, P. S. & McClintock, P. V. E. [2000] "Vibrational resonance," *J. Phys. A: Math. Gen.* **33**, L433-L438.
- Li, J. H. [2002] "Effect of asymmetry on stochastic resonance and stochastic resonance induced by multiplicative noise and by mean-field coupling," *Phys. Rev. E* **66**, 031104-1-7.
- Ullner, E., Zaikin, A., Garcia-Ojalvo, J., Bascones, R. & Kurths, J. [2003] "Vibrational resonance and vibrational propagation in excitable systems," *Phys. Lett. A* **312**, 348-354.
- Wio, H. S. & Bouzat, S. [1999] "Stochastic resonance: The role of potential asymmetry and nonGaussian noises," *Braz. J. Phys.* **29**, 136-143.